



AERODYNAMIC COEFFICIENTS OF A SKI-JUMPER

A.R. Podgayets*, R.N. Rudakov*, V.S. Tuktamishhev*, R.S. Kerov**, B.S. Shvetsov**

* Department of Theoretical Mechanics, Perm State Technical University, 29a, Komsomolskii Prospect, 614600, Perm, Russia, e-mail: rn@tneormech.pstu.ac.ru

** Sport Children and Youth School of Olympic Reserve "Flying Skier", 77-3, Gorkii Street, 614000, Perm, Russia

Abstract. This article is dedicated to finding of ski-jumper's aerodynamic coefficients during the flight. Aerodynamic coefficients are found independently in the mathematical model of airflow around the ski-jumper and by the method of experimental identification with the aid of videorecording of the flight. Both methods are not yet widely used in sport biomechanics but they are rather powerful. The finding of aerodynamic coefficients gives way to a more precise and individual mathematical modeling of the ski-jump which is demonstrated on several examples of optimization of the jump.

Key words: ski jump, aerodynamic coefficients, flight, optimization

Introduction

The basic problem in the mathematical modeling of the jump is finding the aerodynamic coefficients of skier-on-skis system. Experimental studies are known in this problem [1]. The aerodynamic coefficients are found for flight postures of 1950-s and 1960-s. Authors [2, 3] measured aerodynamic quality of a dummy in a V-style posture in a tunnel tube. Unfortunately they did not show aerodynamic coefficients and knowing of aerodynamic quality is not sufficient for a mathematical modeling of the flight. Aerodynamic coefficients were found theoretically in the papers [4-6] on the basis of simple models of airflow around the ski-jumper. This paper employs more precise model of airflow around skier-on-skis system in finite difference method in natural variables and in variables of rotor and flow function. Improved model of ski-jumper is considered in 2D statement and a try is made to take artificially into account the effect of the 3rd direction. Aerodynamic coefficients are also found from processing of videorecording of ski-jumps by the method explained in [7]. Some problems are also solved with the use of aerodynamic coefficients found.

Aerodynamic coefficients

Flying body is affected by full aerodynamic force which is defined by integration of surface stress $\sigma = -pE + 2\mu\xi$ over closed surface of skier-on-skis system Γ_S

$$\mathbf{F} = - \oint_{\Gamma_S} p \mathbf{n} ds + 2 \oint_{\Gamma_S} \mu \xi \cdot \mathbf{n} ds \quad (1)$$

where p is the hydrostatic pressure, E is the unit tensor, μ is the dynamic viscosity of air and ξ is the tensor of the deformation rates with components $\xi_{ij} = \frac{1}{2} \left(\frac{\partial V_i}{\partial x^j} + \frac{\partial V_j}{\partial x_i} \right)$, $i=1,2$ in two dimensions.

Projections of full aerodynamic force on tangent and normal lines are called the force of drag \mathbf{R} directed opposite to the velocity and the force of lift directed perpendicular to velocity:

$$\begin{cases} R = F \sin \alpha = \frac{1}{2} \rho S c_D V^2, \\ Q = F \cos \alpha = \frac{1}{2} \rho S c_L V^2, \end{cases} \quad (2)$$

where ρ is the density of airflow, c_D , c_L are the aerodynamic coefficients, V is the velocity of airflow, S is the area of triangle wing formed by the skier and skis. This meaning of middle section is traditional in aerodynamics of the flight. The original meaning of middle section could not be used so comfortably because it depends on the attack angle.

Equation (1) shows that calculation of aerodynamic forces requires knowing the fields of pressures and velocities around the ski-jumper. They could be obtained from the problem of airflow around the skier-on-skis system.

Mathematical model of airflow in natural variables

Let us consider this problem in 2D statement. Let us choose a square region with the side L so that the effect of skier on the airflow would be negligible on the boundary of the region. Let us introduce the following terms (see Fig. 1.): G is the considered area including its boundary and model of skier-on-skis system, Γ_A is the outer boundary of this area, G_p is the area covered by the model of skier and skis including its boundary and Γ_p is the boundary of the model. The origin of coordinates is situated in the lower left corner of the square and coordinate axes are directed along the sides of the square. It is assumed that the hill does not affect the aerodynamics of the ski-jumper significantly. This assumption is based on a well-known estimation that screen effect takes place within the distance from the ground equal to one third of the length of the body [8]. For a ski-jumper this distance is about 75-85 cm. The ski-jumper terminates the flight and prepares for the landing as long as he reaches such height [2].

The ski-jumper is assumed to stay in the center of the area and the airflow is moving around him. The skier-on-skis is oriented so that skis are parallel to the side of the considered square area. The mathematical model is designed to take into account individual form of each sportsman but current paper uses more general representation of human body as a profile constructed by a combination of arcs and lines (see Figs. 1, 2, 3).

The air is considered as a linear-viscous incompressible liquid because linear model of viscosity best fits for describing of air [9] and compressibility of the air is negligible for the velocities of the skier. Non-stationary flow of a linear-viscous incompressible liquid in the area G is described by equation of Navier-Stokes and condition of incompressibility [10]:

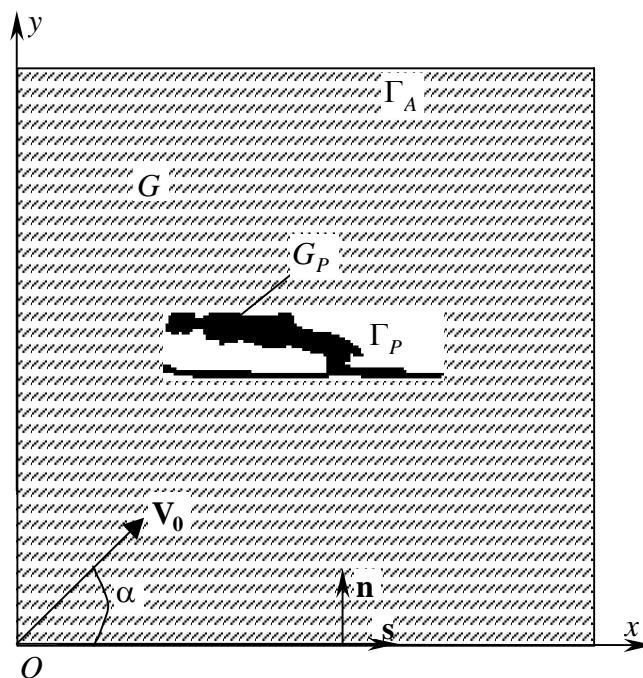


Fig. 1. Boundary conditions for the problem of airflow around skier-on-skis system.



Fig. 2. Photograph of flying ski-jumper (Masahiko Harada, 1998).

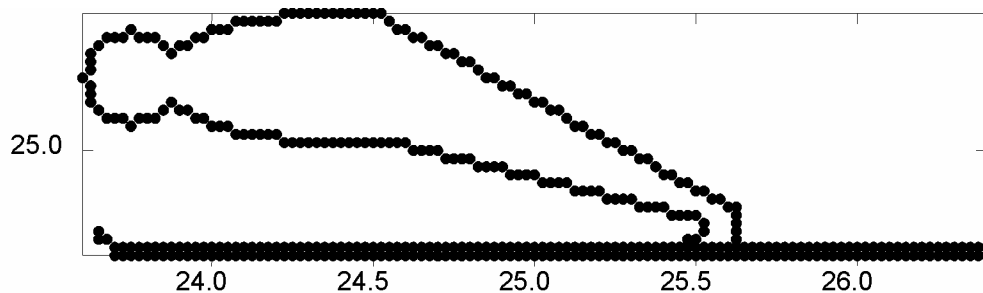


Fig. 3. The form of the profile of skier-on-skis systems for a grid step $h = 0.025$ m.

$$\begin{aligned} \frac{\partial u}{\partial t} + u \frac{\partial u}{\partial x} + v \frac{\partial u}{\partial y} &= -\frac{1}{\rho} \frac{\partial p}{\partial x} + \eta \left(\frac{\partial^2 u}{\partial x^2} + \frac{\partial^2 u}{\partial y^2} \right), \\ \frac{\partial v}{\partial t} + u \frac{\partial v}{\partial x} + v \frac{\partial v}{\partial y} &= -\frac{1}{\rho} \frac{\partial p}{\partial y} + \eta \left(\frac{\partial^2 v}{\partial x^2} + \frac{\partial^2 v}{\partial y^2} \right), \\ \frac{\partial u}{\partial x} + \frac{\partial v}{\partial y} &= 0. \end{aligned} \quad (3)$$

Initial conditions describe undisturbed flow:

$$u(x, y, 0) = V_0 \cos \alpha, \quad v(x, y, 0) = V_0 \sin \alpha, \quad (x, y) \in G \cap G_P, \quad (4a)$$

$$p(x, y, 0) = 0, \quad (x, y) \in G \cap G_P; \quad (4b)$$

conditions on the boundary of the area of calculation Γ_A also correspond to undisturbed flow:

$$u(x, y, t) = V_0 \cos \alpha, \quad v(x, y, t) = V_0 \sin \alpha, \quad (x, y) \in \Gamma_A; \quad (5a)$$

$$p(x, y, t) = 0, \quad (x, y) \in \Gamma_A; \quad (5b)$$

and non-slip boundary condition is stated on the profile of skier-on-skis system:

$$u(x, y, t) = 0, \quad v(x, y, t) = 0, \quad p(x, y, t) = p_S(x, y, t), \quad (x, y) \in \Gamma_P. \quad (6)$$

The problem (3) with boundary conditions (4)-(6) is solved by direct Navier-Stokes (DNS) method [11]. It means that all the area is described in the same way and numerical algorithm is applied to the whole area. Boundary conditions on the profile are satisfied automatically in this approach. A widely used modification of DNS is used in which solid body is considered as an area with infinite volume force [12]. Then equations (3) look as follows:

$$\frac{\partial u}{\partial t} + u \frac{\partial u}{\partial x} + v \frac{\partial u}{\partial y} = -\frac{1}{\rho} \frac{\partial p}{\partial x} + \eta \left(\frac{\partial^2 u}{\partial x^2} + \frac{\partial^2 u}{\partial y^2} \right) - \frac{F}{\rho}, \quad (7a)$$

$$\frac{\partial v}{\partial t} + u \frac{\partial v}{\partial x} + v \frac{\partial v}{\partial y} = -\frac{1}{\rho} \frac{\partial p}{\partial y} + \eta \left(\frac{\partial^2 v}{\partial x^2} + \frac{\partial^2 v}{\partial y^2} \right) - \frac{F}{\rho}, \quad (7b)$$

$$\frac{\partial u}{\partial x} + \frac{\partial v}{\partial y} = 0, \quad (7c)$$

$$F = \begin{cases} \infty, & x \in G_P, \\ 0, & x \in G \cap G_P; \end{cases} \quad (7d)$$

initial conditions are transformed into

$$u(x, y, 0) = V_0 \cos \alpha, \quad v(x, y, 0) = V_0 \sin \alpha, \quad (x, y) \in G, \quad (8a)$$

$$p(x, y, 0) = 0, \quad (x, y) \in G, \quad (8b)$$

and conditions (6) are satisfied automatically.

Equations (7) with initial condition (8) and boundary condition (5) are solved by the method of transition to a steady state. Each iteration by time consists of three sequential steps [13]. It is assumed on the first step that momentum is transferred only by convection and diffusion. Resulting field of velocities does not satisfy condition of incompressibility but it gives right picture of curl characteristics. The aim of the second step is to find a field of pressures with the help of intermediate field of velocities. The second step transfers momentum only by pressure gradients.

It was found that finding of pure pressure $p(t, x, y)$ makes the whole approach unstable so a method used in [14] is used. The author of that paper introduce a “small parameter” – additional pressure $\delta p(x, y)$ which is determined from solution of differential equation

$$\frac{\partial^2 \delta p}{\partial x^2} + \frac{\partial^2 \delta p}{\partial y^2} = \frac{\rho}{\Delta t} \left(\frac{\partial u_2}{\partial x} + \frac{\partial v_2}{\partial y} \right), p(0, x, y) = p_0, p(t, \Gamma_A) = p_0, \quad (9)$$

where subscript “2” marks the variables found in the first step. The field $\delta p(x, y)$ found from (9) allows to correct the distribution of components of velocity vector which now satisfy the equation of incompressibility,

$$\begin{aligned} u(\hat{t}, x, y) &= u_1(\hat{t}, x, y) - \frac{\Delta t}{\rho} \frac{\partial}{\partial x} \delta p(x, y), \\ v(\hat{t}, x, y) &= v_1(\hat{t}, x, y) - \frac{\Delta t}{\rho} \frac{\partial}{\partial y} \delta p(x, y) \end{aligned} \quad (10)$$

and pressure

$$p(\hat{t}, x, y) = p(t, x, y) + \delta p(x, y). \quad (11)$$

$\delta p(x, y)$ in (9) is also found as a stationary limit of a non-stationary solution of a parabolic equation

$$\begin{aligned} \frac{\partial \phi}{\partial \tau} &= \lambda \left(\frac{\partial^2 \phi}{\partial x^2} + \frac{\partial^2 \phi}{\partial y^2} \right) - \frac{1}{\Delta t} \left(\frac{\partial u_2}{\partial x} + \frac{\partial v_2}{\partial y} \right), \\ \phi(0, x, y) &= 0, \phi(t, 0, y) = \phi(t, L, y) = \phi(t, x, 0) = \phi(t, x, H) = 0, \end{aligned} \quad (12)$$

where $\phi = \frac{1}{\lambda p} \delta p$, $\lambda = const$. Parameter λ is used for better stability of numerical algorithm.

In order to use lesser computer memory equations (7a), (7b) and (12) are split by space variables [15]. The resulting algorithm consists of cyclic solution of six one-dimensional equations with three-diagonal matrices.

Split method will be demonstrated in equation (7a). Let us introduce the following terms:

$$A_x(u) = u \frac{\partial}{\partial x} - \eta \frac{\partial^2}{\partial x^2}, A_y(v) = v \frac{\partial}{\partial y} - \eta \frac{\partial^2}{\partial y^2}, f_x(u) = -\frac{1}{p} \frac{\partial p}{\partial x} + c_s V u.$$

The first equation of system (7) could be rewritten as

$$\frac{\partial u}{\partial t} + A_x(u)u + A_y(v)u = f_x(u). \quad (13)$$

We assume that solution $u(t, x, y)$ of equation (13) for the moment of time t is known. Then solution of (13) for a moment $\hat{t} = t + \Delta t$ can be written as

$$u(\hat{t}, x, y) = (E - \Delta t A_x(u) - \Delta t A_y(v))u(t, x, y) + \Delta t f_x(u) + O(\Delta t^2). \quad (14)$$

Let us consider two auxiliary problems:

$$\frac{\partial u_1}{\partial t} + A_x(u)u_1 = f_x(u_1), u_1(t, x, y) = u(t, x, y), u_1(t, 0, y) = u_1(t, L, y) = u_0 \quad (15)$$

$$\frac{\partial u_2}{\partial t} + A_y(v)u_2 = 0, u_2(t, x, y) = u_1(\hat{t}, x, y), u_1(t, x, 0) = u_1(t, x, H) = u_0. \quad (16)$$

Solutions of these problems for the moment of time $\hat{t} = t + \Delta t$ can be presented:

$$u_1(\hat{t}, x, y) = (E - \Delta t A_x(u))u_1(t, x, y) + \Delta t f_x(u_1) + O(\Delta t^2), \quad (17)$$

$$u_2(\hat{t}, x, y) = (E - \Delta t A_y(v))u_2(t, x, y) + O(\Delta t^2). \quad (18)$$

Regarding these formulas and initial conditions the solution of auxiliary problem (16) can be written in the following form:

$$u_2(\hat{t}, x, y) = (E - \Delta t A_y(v)) \cdot \left[(E - \Delta t A_x(u)) u_1(t, x, y) + \Delta t f_x(u_1) + O(\Delta t^2) \right] + O(\Delta t^2). \quad (19)$$

Multiplication of expressions inside square brackets leads us to

$$u_2(\hat{t}, x, y) = (E - \Delta t A_x(u) - \Delta t A_y(v)) u(t, x, y) + \Delta t f_x(u) + O(\Delta t^2). \quad (20)$$

The last expression takes into account initial conditions of the first auxiliary problem. Comparison of (20) with (14) allows us to state that sequential solution of one-dimensional problems (15) and (16) gives the solution of equation of (7a) with error not higher than $O(\Delta t^2)$. Neumann's stability analysis of coefficients of run method shows that equation (15) is absolutely stable and (16) is stable except the case when the speed is larger than 1 and strictly vertical or horizontal. But numerical experiments showed that instability does not appear in this case, too.

Separated finite difference grid with step h is used for approximation of equations on the considered square with length L . Nodes of the grid are numerated from 0 to $N+1$. Scheme against the flow is used. Finite difference approximation will be demonstrated in equation (15):

$$\frac{\partial u_1}{\partial t} + u \frac{\partial u_1}{\partial x} - \eta \frac{\partial^2 u_1}{\partial x^2} = -\frac{1}{\rho} \frac{\partial p}{\partial x} + c_s V u. \quad (21)$$

Replacing the derivatives in (21) by their finite differences gives us the following:

$$\begin{cases} \frac{\hat{u}_{ij} - u_{ij}}{\Delta t} + \frac{u_{ij}(\hat{u}_{ij} - \hat{u}_{i-1j})}{h} - \frac{\eta(\hat{u}_{i+1j} - 2\hat{u}_{ij} + \hat{u}_{i-1j})}{h^2} = -\frac{p_{ij} - p_{i-1j}}{\rho h} + c_s V u, & u \geq 0, \\ \frac{\hat{u}_{ij} - u_{ij}}{\Delta t} + \frac{u_{ij}(\hat{u}_{i+1j} - \hat{u}_{ij})}{h} - \frac{\eta(\hat{u}_{i+1j} - 2\hat{u}_{ij} + \hat{u}_{i-1j})}{h^2} = -\frac{p_{ij} - p_{i-1j}}{\rho h} + c_s V u, & u < 0. \end{cases} \quad (22)$$

Let us transform these expressions for the realization of run method:

$$\begin{cases} \hat{u}_{i-1} \left(-\frac{u_{ij}}{h} - \frac{\eta}{h^2} \right) + \hat{u}_i \left(\frac{1}{\Delta t} + \frac{u_{ij}}{h} + 2\frac{\eta}{h^2} \right) + \hat{u}_{i+1} \left(-\frac{\eta}{h^2} \right) = \frac{u_{ij}}{\Delta t} - \frac{p_{ij} - p_{i-1j}}{\rho h} + c_s V u, & u \geq 0, \\ \hat{u}_{i-1} \left(-\frac{\eta}{h^2} \right) + \hat{u}_i \left(\frac{1}{\Delta t} + \frac{u_{ij}}{h} + 2\frac{\eta}{h^2} \right) + \hat{u}_{i+1} \left(\frac{u_{ij}}{h} - \frac{\eta}{h^2} \right) = \frac{u_{ij}}{\Delta t} - \frac{p_{ij} - p_{i-1j}}{\rho h} + c_s V, & u < 0. \end{cases} \quad (23)$$

Analysis of approximation of (23) shows that members of discrepancy with the first order of error cancel each other when two directions (15) and (17) are added together so that resulting finite difference equations have second order of approximation by time and space coordinates [16]. This scheme is also conservative and boundary conditions of Dirichlet does not reflect disturbances [17] thus allowing more precise modeling of physical processes in the airflow.

Numerical experiments showed that sufficient parameters of the grid for mathematical modeling of airflow around skier-on-skis system are square 50*50 m ($L=50$ m) and number of nodes $N=2000$ over each of coordinate axes ($h=2.5$ cm). A modification of multi-grid method based on shrinking of the area after the airflow becomes steady is used to fit the fields of variables in RAM. Numerical experiments provided conditions when it could be done without change in aerodynamic coefficients. One computation of aerodynamic coefficients for a given attack angle required about 8-12 hours on a Celeron-533 computer with 64 MB of RAM.

In order to give exit for the air that goes between the skier and skis, the legs of the skier were made penetrable. The value of volume force was chosen from the condition of minimal discrepancy between experimental and calculated flight distance for a given ski-jumper. Thus a coefficient of resistance of skier's legs was determined: $c_s=0,1 \text{ N/m}^3$.

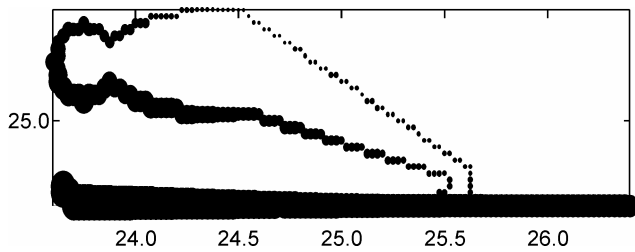


Fig. 4. Pressure on the profile for $v=25$ m/c and $\alpha=30^\circ$. Scale: maximal pressure ● – 250 Pa, minimal pressure • – -134 Pa. Skis model is two nodes wide. The second row of grid nodes is artificially shown lower.

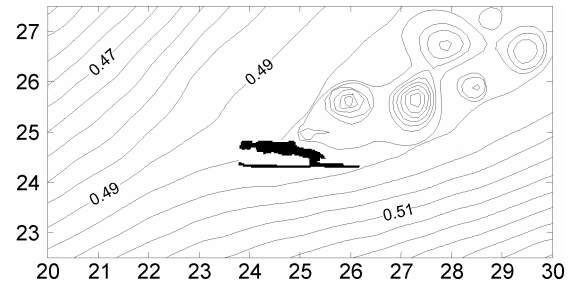


Fig. 5. Flow functions in the part of area of calculation around the ski-jumper for $v=25$ m/c and $\alpha=30^\circ$.

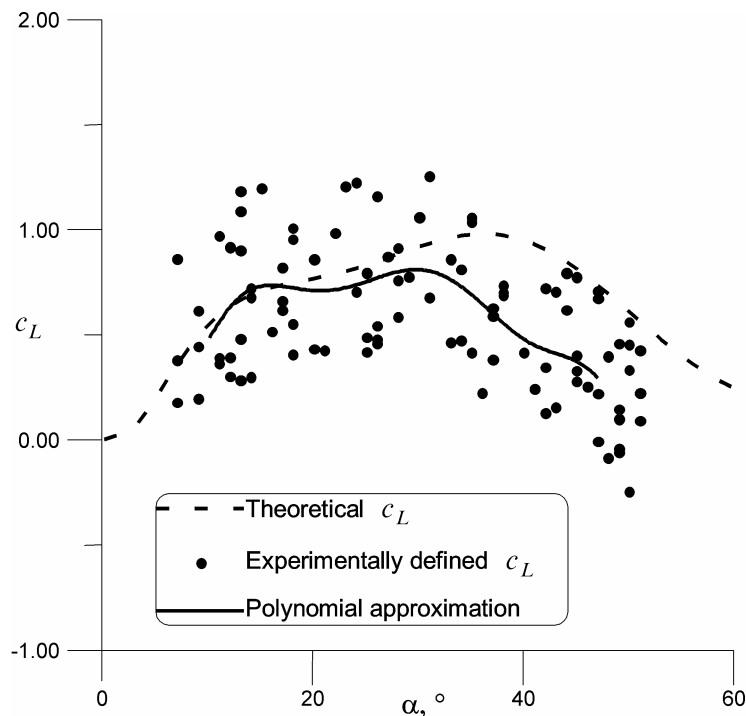


Fig. 6. Aerodynamic coefficient of lift found from experimental identification of movement videorecording.

Fig. 4 shows the diagram of pressure on the profile of skier-on-skis system. A strong rarefaction is observed after the ski-jumper. The main pressure lies on skis, helmet and breast of the sportsman.

Fig. 5 shows field of flow functions around the ski-jumper. Carman's curl track is seen rather well. Despite the fact that turbulence was not taken into account in the mathematical statement of the problem, full equations of Navier-Stokes allowed to describe the most large curls. Non-symmetry appears even for attack angles 0° and 90° . It is caused not by turbulent pulsation certainly but by pulsation of numerical instability. Despite this fact the resulting picture of airflow around the ski-jumper is alike pictures of underersonic airflow around other bodies with complex form.

Dashed line on Figs. 6, 7 shows aerodynamic coefficients found from this problem.

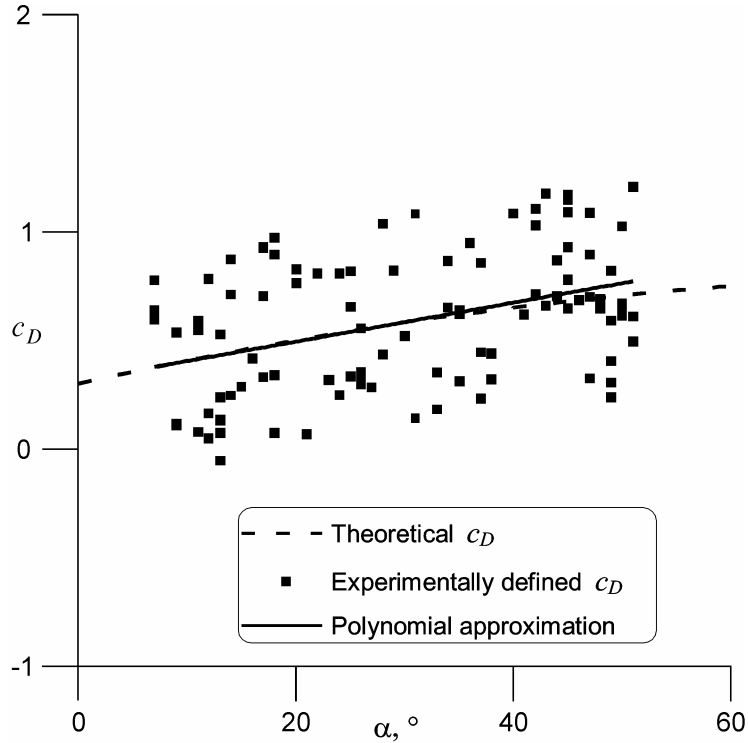


Fig. 7. Aerodynamic coefficient of drag found from experimental identification of movement videorecording.

Solution of the problems in the variables curl – flow function

Flow function ψ and curl φ are defined as follows [10]:

$$u = \frac{\partial \psi}{\partial y}, \quad v = -\frac{\partial \psi}{\partial x}, \tag{24a}$$

$$\varphi = \text{rot } \mathbf{V}. \tag{24b}$$

Let us differentiate equation (7a) with respect to y and equation (7b) with respect to x . Adding them one to another leads us to Navier-Stokes equation in flow function – curl variables:

$$\frac{\partial \varphi}{\partial t} = -u \frac{\partial \varphi}{\partial x} - v \frac{\partial \varphi}{\partial y} + \nu \frac{\partial^2 \varphi}{\partial x^2} + \nu \frac{\partial^2 \varphi}{\partial y^2} - c_s V^2 \varphi + c_s A, \tag{25}$$

where

$$A = \left(\frac{\partial^2 \psi}{\partial x^2} \left(\frac{\partial \psi}{\partial x} \right)^2 + 2 \frac{\partial \psi}{\partial x} \frac{\partial \psi}{\partial y} \frac{\partial^2 \psi}{\partial x \partial y} + \frac{\partial^2 \psi}{\partial y^2} \left(\frac{\partial \psi}{\partial y} \right)^2 \right). \tag{26}$$

Equation (24b) can be rewritten as Poisson’s equation for ψ :

$$\Delta \psi = -\varphi. \tag{27}$$

Let us differentiate (7a) with respect to x and equation (7b) with respect to y . Adding them one to another and considering the condition of incompressibility (7c) and (24) gives us equation of Poisson for pressure:

$$\frac{\partial^2 p}{\partial x^2} + \frac{\partial^2 p}{\partial y^2} = 2 \frac{\partial^2 \psi}{\partial x^2} \frac{\partial^2 \psi}{\partial y^2} - 2 \left(\frac{\partial \psi}{\partial x \partial y} \right)^2. \tag{28}$$

Here p is unknown variable and ψ is known.

Table 1. Boundary conditions for φ and ψ .

Boundary	Condition on ψ	Condition on φ
Lower	$\psi_{i0} = vih + uH,$	$\varphi_{i0} = \frac{2}{h^2}(vih + uH - \psi_{i1}) - \frac{2}{h}u,$
Right	$\psi_{N+1j} = vL + uH - ujh,$	$\varphi_{N+1j} = \frac{2}{h^2}(vL + uH - ujh - \psi_{Nj}) - \frac{2}{h}v,$
Upper	$\psi_{iN+1} = vih,$	$\varphi_{iN+1} = \frac{2}{h^2}(vih - \psi_{iN}) + \frac{2}{h}u,$
Left	$\psi_{0j} = uH - ujh,$	$\varphi_{0j} = \frac{2}{h^2}(uH - ujh - \psi_{1j}) + \frac{2}{h}v,$
Initial condition	$\psi_{ij} = vih + uH - ujh,$ $i, j = \overline{0, N+1}.$	$\varphi_{ij} = 0,$ $i, j = \overline{0, N+1}.$

Boundary conditions are stated over natural axis that goes along the sides of the square area from its lower left corner against clockwise (see Fig. 1). Initial value of flow function is taken $\psi_0 = uH$ to make it positive in all area. Boundary conditions for curl are determined by the formula of Thom [10]. Boundary equations for pressure are similar to those in previous problem (5b). Initial conditions describe stationary solution of undisturbed airflow through considered area. In this case curl is zero, flow functions are lines with angle to the horizontal equal to the attack angle and pressure is the same in every point of the area (4b). Boundary conditions for curl and flow function are written in Table 1. Boundary conditions for pressure are (4b), (8b).

A finite difference grid with step h is used to approximate equations (25)-(28) in the square area with the side L . Grid nodes are numerated from 0 to $N+1$. Central finite differences were chosen to approximate original equations.

Computational process is organized in the following way.

1. Initial conditions (Table 1, (4b)) are put on curl, flow function and pressure.
2. Navier-Stokes equation (25) is solved in order to find curl in internal nodes of considered area. Curl on the boundary is taken from the previous step. A split method [18] is used to solve equation (25): the first step is designed to solve equation (25) for spreading the curl along x -axis (see boundary conditions in Table 1):

$$\frac{\tilde{\varphi} - \varphi}{\Delta t / 2} = -u \frac{\partial \tilde{\varphi}}{\partial x} - v \frac{\partial \varphi}{\partial y} + \nu \frac{\partial^2 \tilde{\varphi}}{\partial x^2} + \nu \frac{\partial^2 \varphi}{\partial y^2} - c_s V^2 \tilde{\varphi} + c_s A, \quad (29)$$

where $\tilde{\varphi}$ is the new curl of the first step. Finite difference approximation of (29) is as follows:

$$\begin{aligned} \tilde{\varphi}_{i+1j} \left(\frac{\psi_{ij+1} - \psi_{ij-1}}{4h^2} + \frac{v}{h^2} \right) + \tilde{\varphi}_{ij} \left(-\frac{2}{\Delta t} - \frac{2v}{h^2} + c_s V^2 \right) + \tilde{\varphi}_{i-1j} \left(-\frac{\psi_{ij+1} - \psi_{ij-1}}{4h^2} + \frac{v}{h^2} \right) = \\ = -\frac{2\varphi_{ij}}{\Delta t} + \frac{\psi_{i+1j} - \psi_{i-1j}}{2h} \frac{\varphi_{ij+1} - \varphi_{ij-1}}{2h} - \nu \frac{\varphi_{ij+1} - 2\varphi_{ij} + \varphi_{ij-1}}{h^2} + c_s A. \end{aligned} \quad (30)$$

Then curl is spread only along y -axis of the second step:

$$\frac{\hat{\varphi} - \tilde{\varphi}}{\Delta t / 2} = -u \frac{\partial \tilde{\varphi}}{\partial x} - v \frac{\partial \hat{\varphi}}{\partial y} + \nu \frac{\partial^2 \tilde{\varphi}}{\partial x^2} + \nu \frac{\partial^2 \hat{\varphi}}{\partial y^2} - c_s V^2 \hat{\varphi} + c_s A, \quad (31)$$

where $\hat{\varphi}$ is a new value of curl in the second step. Finite difference approximation of (31) is as follows:

$$\begin{aligned} \hat{\phi}_{ij+1} \left(\frac{\Psi_{ij+1} - \Psi_{ij-1}}{4h^2} + \frac{v}{h^2} \right) + \hat{\phi}_{ij} \left(-\frac{2}{\Delta t} - \frac{2v}{h^2} + c_s V^2 \right) + \hat{\phi}_{ij-1} \left(-\frac{\Psi_{ij+1} - \Psi_{ij-1}}{4h^2} + \frac{v}{h^2} \right) = \\ = -\frac{2\tilde{\phi}_{ij}}{\Delta t} + \frac{\Psi_{i+1j} - \Psi_{i-1j}}{2h} \frac{\tilde{\phi}_{ij+1} - \tilde{\phi}_{ij-1}}{2h} - v \frac{\tilde{\phi}_{ij+1} - 2\tilde{\phi}_{ij} + \tilde{\phi}_{ij-1}}{h^2} + c_s A. \end{aligned} \quad (32)$$

3. Flow function is found in all nodes of the area from solution of equation (24b). Poisson's equation for the flow function is solved by the method of sequential upper relaxation because this method was successfully used in a wide variety of problems and proved to be simple and reliable. Finite difference scheme of this method is following [18]:

$$\hat{\psi}_{ij} = \psi_{ij} + \frac{\omega}{4} \left(h^2 \hat{\phi}_{ij} + \hat{\psi}_{i-1j} + \hat{\psi}_{ij-1} + \psi_{i+1j} + \psi_{ij+1} - 4\psi_{ij} \right), \quad (33)$$

where ω is a relaxation parameter that define convergence speed. For the best convergence in rectangular area with Dirichlet boundary conditions and initial conditions describing undisturbed airflow the following value of ω is recommended [18]: $\omega = \omega_0 = 2 \frac{1 - \sqrt{1 - \xi}}{\xi}$

where $\xi = \cos^2 \frac{\pi}{N}$. For our problem $\omega_0 = \frac{2}{1 + \sin \frac{\pi}{N}}$.

4. New boundary conditions for curl are calculated with the aid of Thom's formula (see Table 1).

5. Pressure is found from Poisson's equation (27) which is solved by method of additional pressure (12),(11),(4b),(8b).

Aerodynamic coefficients found for $L=50\text{m}$ and $N=2000$ differ from aerodynamic coefficients found in the previous problem by the value less than 0.001 (see dashed line in Figs. 6, 7).

Experimental identification of aerodynamic coefficients by videorecording of the flight

The paper [7] suggests a method of experimental determining of aerodynamic coefficients of skier-on-skis system. The following formulas are derived for them:

$$\begin{aligned} Sc_D &= \frac{2m}{\rho v^2} (-a_\tau + g \sin \beta), \\ Sc_L &= \frac{2m}{\rho v^2} (-a_n + g \cos \beta), \end{aligned} \quad (34)$$

where a_τ is the tangent acceleration of a ski-jumper, a_n is the normal acceleration, β is the angle between the horizontal and velocity.

Variables of (34) were approximated by finite differences:

$$v_i = \frac{\Delta l_i}{\Delta t}, \quad a_{\tau,i} = \frac{v_{i+1} - v_i}{\Delta t}, \quad \beta_i = \arcsin \frac{\Delta y_i}{\Delta l_i}, \quad a_{n,i} = \frac{v_i \sin(\beta_{i+1} - \beta_i)}{\Delta t}. \quad (35)$$

The experiment was made to test this method. Experiment took place on the basis of Perm SCYSOR "Flying Skier" in January 2002. Camera capable of making 50 shots per second was placed 20 m away from the plane of the flight and was oriented horizontally perpendicular to the plane of the flight. Videorecording of eight jumps of ski-jumpers 9-15 years old was made. Masses of sportsmen with their equipment and lengths of skis were also measured. Then videorecording was coded to .AVI format and processed by CorelDraw graphics editor. Only moments when flight posture did not change were used for further analysis. Relative movements of center of mass of the skier between shots were determined.

Time scale was determined by the time of the whole flight and coordinate scale was determined by the length of skis. Computer helped to reduce measurement error to 0.3 mm. Unfortunately, such error of measurement on the screen of computer produced error of determining of aerodynamic coefficients (34)-(35) 5 % - 100 % and more.

The problem of determining the aerodynamic characteristics of flying body by the videorecording of movement is known in literature (e.g., [19]). The idea of these approaches is to take into account the error of measurement by methods of mathematical statistics with the aid of some hypothesis on the kind and parameters of distribution of the error. Then kind of dependences of aerodynamic coefficients on the attack angle is determined and parameters of these approximations are chosen from some condition of "quality" of results. In order to improve or at least to ensure convergence different mathematical methods are used. Usually they does not give significant increase in results, main factor remains the quality of experiment. That is why we used only "pure" approach of experimental identification. After processing we obtained about three hundreds of values of aerodynamic coefficients. After selecting the moments of time, when the posture of the ski-jumper did not change and adding measurement error to original data produced change of aerodynamic coefficients less than 30 %, we have got 117 values of c_D and c_L . Let us present every value of aerodynamic coefficients as $z_i = g_i + w_i$, where z_i is a value number i with error, g_i is a true value of aerodynamic coefficient, and w_i is measurement error. We have more than hundred of values for each coefficients, so we can suggest that distribution of measurement error is normal with zero expected value according to central limit theorem of Lyapunov. The approximation functions for aerodynamic coefficients were chosen to be polynomials. The algorithm of identification is following:

Let us choose the power of approximating polynomials.

Random errors with given distribution are subtracted from known values z_i . A normal distribution of error was used with zero expected value and variance equal to variance of sample of aerodynamic coefficients for a given attack angle.

Coefficients of polynomials were calculated by method of minimal squares.

Discrepancy of calculated distance from real distance was calculated with the use of aerodynamic coefficients defined in step 3.

Steps 2-4 are repeated until the sample of discrepancies is representative.

If minimal discrepancy is large then go to step 1.

Table 2. Coefficients of polynomial approximating lift aerodynamic coefficient. N=10.

Power	Value of coefficient
0	$2.256 \cdot 10^1$
1	$-1.030 \cdot 10^1$
2	$2.007 \cdot 10^0$
3	$-2.189 \cdot 10^{-1}$
4	$1.508 \cdot 10^{-2}$
5	$6.950 \cdot 10^{-4}$
6	$2.190 \cdot 10^{-5}$
7	$-4.674 \cdot 10^{-7}$
8	$6.465 \cdot 10^{-9}$
9	$-5.221 \cdot 10^{-11}$
10	$1.864 \cdot 10^{-13}$

Table 3. Coefficients of polynomial approximating drag aerodynamic coefficient. $N = 1$.

Power	Value of coefficient
0	$3.146 \cdot 10^{-1}$
1	$8.965 \cdot 10^{-3}$

Low power polynomial gives big discrepancy of distances because of little number of adjusted parameters and high power polynomial oscillates and gives big discrepancy of distances, too. The dependence of minimal discrepancy (see step 6 in the algorithm of identification) on the power of polynomial is a single-mode function which makes possible finding of global maximum.

The problem of minimization is solved by exhaustive search separately for two aerodynamic coefficients. Coefficients of approximating polynomials are presented in Tables 2,3. Aerodynamic coefficients are presented in Figs. 6, 7. Solid lines present aerodynamic coefficients found from airflow problems. It is seen that completely different methods of determining the aerodynamic coefficients show some similarity.

Problems of optimization in ski-jumping

The aerodynamic coefficients once known open way for mathematical modeling of the ski-jump. L.P. Remizov solved optimization problem for the attack angle [20-22]. Here this problem is solved in some simpler statements for new aerodynamic coefficients.

Mathematical models of phases of a ski-jump were explained in previous issues of Russian Journal of Biomechanics: acceleration [7], take-off and flight [4], landing [23]. They are based on assumption that the posture of the sportsman does not change during acceleration and flight and such postures as forming flight posture and preparing for landing have only slight effect on flight distance.

Optimization of attack angle

Attack angle is the sum of two angles: $\alpha = \delta + \gamma$, where δ is angle between velocity and horizontal: $\cos \delta = \frac{u}{V}$, $\sin \delta = \frac{v}{V}$, γ is angle between skis and horizontal. Let us assume for simplicity that the angle of skis to the horizontal changes with time as $\gamma(t) = c_0 + c_1 t + c_2 t^2 + c_3 t^3 + \dots + c_N t^N$. Then the problem of optimal control of the flight can be rewritten in the following form:

$$\begin{cases} L(c_0, \dots, c_N) \rightarrow \max_{c_0 \dots c_N}, \\ \alpha(t) \geq 0, \alpha(t) \leq 60, v_n < 3.6. \end{cases} \quad (36)$$

The problem was solved by Nelder-Mid method with $N=3$. It was found that c_3 always is zero, so angle of skis to the horizontal was taken as follows for further investigations:

$$\gamma(t) = \frac{\varepsilon t^2}{2} + \omega t + \varphi_0. \quad (37)$$

Thus optimization problem (36) takes the following form:

$$\left\{ \begin{array}{l} L(x, \varepsilon, \omega, \gamma_0) \rightarrow \max_{\varepsilon, \omega, \gamma_0}, \\ \alpha = \beta + \gamma, \quad \gamma(t) = \frac{\varepsilon t^2}{2} + \omega t + \gamma_0, \\ \beta(t) = \arctg \frac{v_y(t)}{v_x(t)}, \\ \alpha(t) > 0, \quad \alpha(t) < 60, \quad v_n < v_1, \\ |\varepsilon| < 30, \quad |\omega| < 60, \quad |\gamma_0| < 10, \end{array} \right. \quad (38)$$

Solution of the problem (38) is presented in Figs. 8, 9, 10 for a jumping hill K110, Innsbruck, Austria for acceleration distance 55 m.

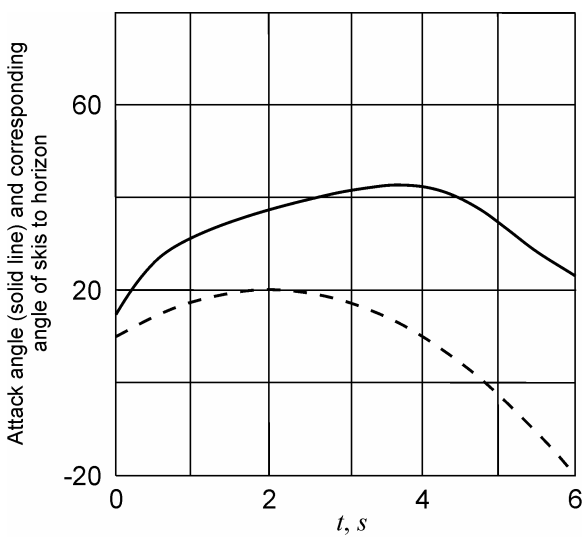


Fig. 8. Example of optimal attack angle for maximal flight distance. Solid line is attack angle. Dashed line is angle of skis to the horizontal.

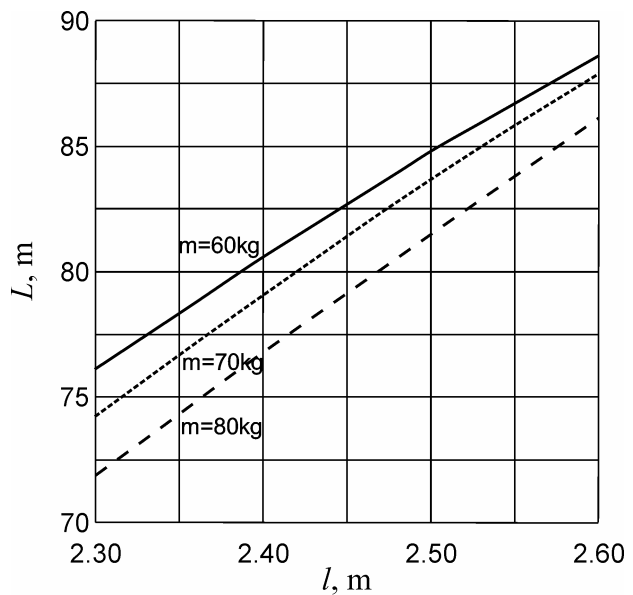


Fig. 9. Dependence of flight distance on skis lengths for different masses of skier-on-skis.

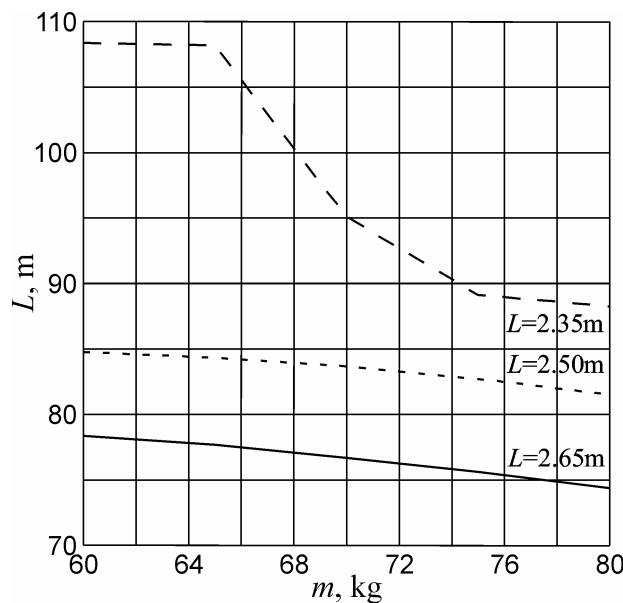


Fig. 10. Dependence of flight distance on mass of skier-on-skis system for different skis lengths.

Optimization of attack angle with disturbances

Let us consider the following situation. The ski-jumper uses optimal tactics but his skis are trembling or wind gust comes. The attack angle is not optimal after that. So it is natural to state the following question: how to behave during the flight if wind gusts and skis tremble are possible.

Such problems can be solved with different approaches but the most simple of them is stochastic optimization [24]. Here is statement of such problem:

$$\begin{cases} L(x, \gamma^*(t)) \rightarrow \max_{\gamma^*(t)}, \\ P\left(\max_t |\gamma(t) - \gamma^*(t)| < \delta_\gamma\right) \geq P^{**}, \quad P\left(\max_t |u(t)| < \delta_u\right) \geq P^{**}, \quad P\left(|L - L^*| < \varepsilon_L\right) \geq P^*, \\ \gamma(t) \geq 0, \quad \gamma(t) \leq 60, \quad v_n < 3,6. \end{cases} \quad (39)$$

Here $\gamma^*(t)$ is an angle from expression (37). It is actual parameter of optimization. But factual angle of skis to the horizontal is affected by skis tremble of random magnitude and period $\gamma(t) = \gamma^*(t) + a_\gamma \sin\left(t_\gamma \frac{T_\gamma}{2\pi}\right)$ and by wind gusts. P^* and P^{**} are confidence levels and δ_γ , δ_u , ε_L are confidence intervals. Stochastic optimization problem is reduced to determinate optimization problem in the following way:

Get representative sample of flight distances for different realizations of random variables in (39).

Determine confidence levels of distance, angle and wind velocity ($P^* = P^{**} = 0.99$). Make confidence level of distance ε_L equal to given (1.00±0.05 m). To make it the step 1 is repeated.

Calculate initial value of optimization criterion. In this paper it is calculated as expected value of distances in the sample. Adjust it with respect to the constraints. Find confidence intervals of angle δ_γ and wind speed δ_u .

Determinate optimization problem is solved by Nelder-Mid method. The results of stochastic optimization are presented in Figs. 11, 12, 13.

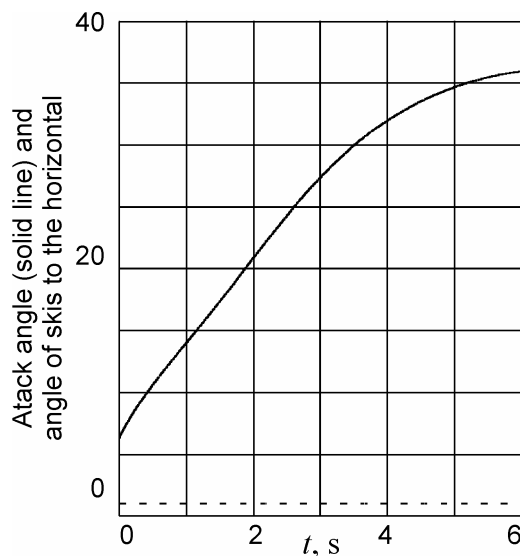


Fig. 11. Stochastic optimal attack angle (solid line) and corresponding angle of skis to the horizontal (dashed line).

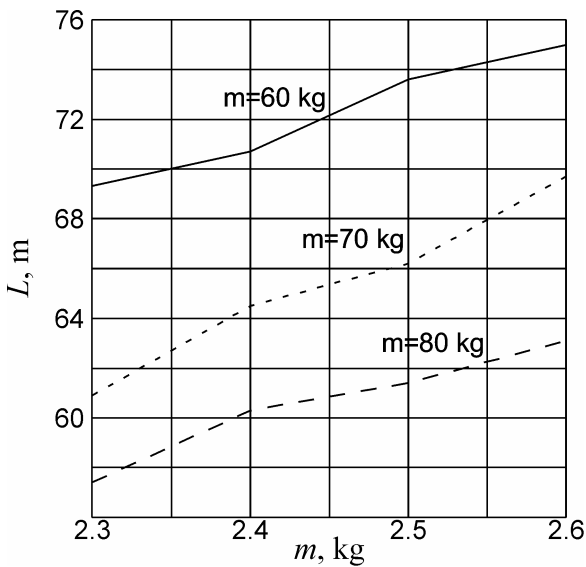


Fig. 12. Dependence of flight distance on skis lengths for different masses of skier-on-skis.

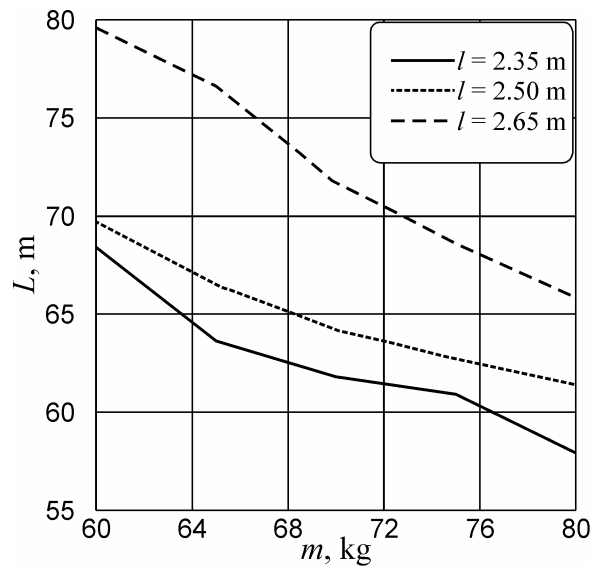


Fig. 13. Dependence of flight distance on mass of skier-on-skis system for different skis lengths.

Stochastic optimal tactics is the tactics that is used now. Wind gusts and skis tremble are more dangerous for light skiers, sometimes constraints on attack angle can be broken because of disturbances during the flight. Generally stochastic attack angles are much higher than determinate optimal.

Optimal mass of skier-on-skis system for a known acceleration length

It is known that different jumping hills and different competitions on the same jumping hill give advantage to different ski-jumpers. It is partially caused by different acceleration length. Let us answer the question: the skier of what mass will flight the most long distance if all the competitors use optimal tactics for maximizing the flight distance? Its mathematical statement is as follows:

$$\begin{cases} L(s, m) \rightarrow \max_m, \\ L(s, m) = \max_{\gamma(t)} L(s, m, \gamma(t)). \end{cases} \quad (40)$$

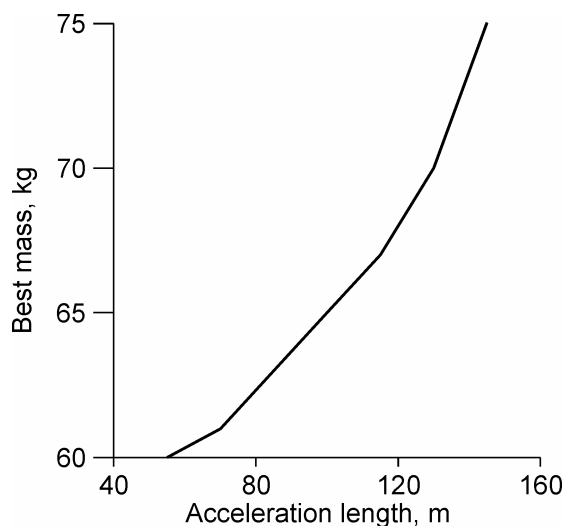


Fig. 14. Optimal mass of skier-on-skis system for different acceleration length on a K110 jumping hill in Innsbruck, Austria.

This is a single variable problem of optimization, it is solved by the method of halving the interval. Optimization criterion is solution of previous problem. The solution of this problem is presented in Fig. 14.

It is seen that long acceleration run gives advantage to heavy ski-jumpers (or ski-jumpers with heavy equipment). As analysis of trajectory shows, the difference of distances between the jumpers that use optimal tactics of the flight would be about 0.5-1 m, but it is enforced by the fact that light ski-jumpers are more affected by random factors of the flight (such as slight wind gusts) and can change the outcome of competitions.

Conclusions

The problems of optimization are more for demonstrating the possibilities of implementing the aerodynamic coefficients: they are based on rather simple mathematical models of phases of the jump that does not take into account movements of sportsman in each phase. Solution of more serious optimization problems is the topic of future works.

Despite the fact that airflow problem was solved in a 2D statement aerodynamic coefficients found from it showed good match with aerodynamic coefficients found by experimental identification method and give some match with real results of the jumps. We hope that aerodynamic coefficients and methods of their finding published in this work will be used for further refining of the style of a ski-jump.

References

1. Грозин Е.А. **Прыжки с трамплина**. М., Физкультура и спорт, 1971 (in Russian).
2. Боженинов О.М., Жилияков А.А. **Основные направления совершенствования техники прыжка на лыжах**. М., ЦНИС, 1993 (in Russian).
3. Боженинов О.М. Факторы, влияющие на результат в прыжках с трамплина на лыжах и эволюцию техники полёта. **Теория и практика физической культуры**, 1: 37-40, 1995 (in Russian).
4. Nyashin Y. I., Podgayets A. R., Rudakov R. N. Mechanics of a Ski Jump. **Russian Journal of Biomechanics**, 2(1-2): 89-97, 1998.
5. Подгаец А. Р., Рудаков Р. Н. Биомеханические проблемы прыжка на лыжах с трамплина. **Российский журнал биомеханики**, 4(2): 20-30, 2000 (in Russian).
6. Podgayets A.R., Rudakov R.N., Tuktamishhev V.S. Aerodynamic optimization of a ski jump. Proceedings of IV International Conference on the Engineering of Sport, Ujihashi S., Haake S.J. (Editors), Oxford, Blackwell Science, 415-422, 2002.
7. Rudakov R.N., Nyashin Yu.I., Podgayets A.R., Lisovski A.F., Miheeva S.A. The influence of aerodynamic forces on the movement of sportsmen and sport balls. **Russian Journal of Biomechanics**, 5(2): 83-94 – 2001.
8. **Аэродинамическая компоновка и характеристики летательных аппаратов**. Сборник статей, М.И. Ништа (Редактор), М., Машиностроение, 1991 (in Russian).
9. Самарский А.А., Арсенин В.Я. О численном решении уравнений газовой динамики с различными типами вязкости. **Журнал вычислительной математики и математической физики**, 1(2): 357-360, 1961 (in Russian).
10. FLETCHER C.A.J. **Computational techniques for fluid dynamics**. Berlin – Heidelberg – New York – London – Paris – Tokyo, Springer Verlag, 1991.
11. Годунов С.К., Семендяев К.А. Разностные методы численного решения задач газовой динамики. **Журнал вычислительной математики и математической физики**, 2(1): 3-14 – 1962 (in Russian).
12. Бояршинов М.Г. **Модели переноса и рассеяния примесей в растительном массиве**. Пермь, ПГТУ, 2000 (in Russian).
13. Белоцерковский О.М. **Численное моделирование в механике сплошных сред**. М., Наука, 1982 (in Russian).
14. Дородницын А.А. Использование метода малого параметра для численного решения уравнений математической физики. В книге: Белоцерковский О.М. (Редактор). **Численные методы решения задач механики сплошных сред**. Курс лекций, прочитанных в летней

- школе в численных методам, г.Киев, 15 июня – 7 июля 1966. М., ВЦ АН СССР, 85-100, 1969 (in Russian).
15. Марчук Г.И. Метод «расщепления» для решения задач математической физики. В книге: Белоцерковский О.М. (Редактор). **Численные методы решения задач механики сплошных сред**. Курс лекций, прочитанных в летней школе в численных методам, г.Киев, 15 июня – 7 июля 1966. М., ВЦ АН СССР, 66-84, 1969 (in Russian).
 16. Бояршинов М.Г. **Численные методы**. Часть 2. Пермь, ПГТУ, 1999 (in Russian).
 17. Дородницын Л.В. Неотражающие граничные условия для систем уравнений газовой динамики. **Журнал вычислительной математики и математической физики**, 42(4): 522-549, 2002 (in Russian).
 18. ROACHE P.J. **Computational fluid dynamics**. Hermosa publishers, Albuquerque, 1976.
 19. Дроздов А.Л. Алгоритм идентификации характеристик динамической системы по данным наблюдений. **Автоматика и телемеханика**, 5: 58-66, 2000 (in Russian).
 20. Remizov L.P. Biomechanics of optimal ski jump. **J Biomechanics**, 3(3): 167-171, 1984.
 21. Ремизов Л.П. Максимальная дальность прыжка с трамплина. **Теория и практика физической культуры**, 3: 73-75, 1973 (in Russian).
 22. Ремизов Л.П. К оптимальной технике прыжка на лыжах с трамплина. **Теория и практика физической культуры**, 10: 79-81, 1980 (in Russian).
 23. Podgayets A.R., Rudakov R.N. Evaluation of the Effect of Ski-Jumper's Aerodynamic Quality on Safety of Landing. **Russian Journal of Biomechanics**, 3(3): 91-98, 1999.
 24. Гитман М.Б. Методика решения задачи стохастической оптимизации технологических процессов обработки металлов при стохастическом распределении начальных условий. **Математическое моделирование систем и процессов**, 1(1): 20-25, 1992 (in Russian).

АЭРОДИНАМИЧЕСКИЕ КОЭФФИЦИЕНТЫ СИСТЕМЫ ЛЫЖНИК-ЛЫЖИ ПРИ ПРЫЖКЕ С ТРАМПЛИНА

А.Р. Подгаец, Р.Н. Рудаков, В.С. Туктамышев, Р.С. Керов, Б.С. Швецов
(Пермь, Россия)

Основной проблемой в математическом моделировании прыжка на лыжах с трамплина является определение аэродинамических коэффициентов системы лыжник-лыжи. Известно экспериментальное определение их в работе [1] для стиля прыжков 1950-х и 1960-х годов. В работах [2,3] обдувался манекен и исследовался современный V-стиль. Однако, в этих работах приводится лишь аэродинамическое качество системы лыжник-лыжи, а для математического моделирования полёта необходимо знать аэродинамические коэффициенты лобового сопротивления и подъёмной силы. В работах [4-6] аэродинамические коэффициенты определялись расчётным способом на основе простейших моделей обтекания лыжника потоком воздуха. В настоящей работе для определения аэродинамических коэффициентов рассматривается более точная модель обтекания системы лыжник-лыжи потоком воздуха с использованием метода конечных разностей в естественных переменных (скорость, давление) и в переменных вихрь, функция тока. Рассматривается достаточно точная конфигурация системы в плоской постановке и искусственно учитывается объёмность задачи. Аэродинамические коэффициенты определяются также путём обработки по методике [7, 8] видеозаписей прыжков с трамплина. В работе приведено также решение некоторых интересных задач с использованием полученных зависимостей аэродинамических коэффициентов от угла атаки. Библ. 24.

Ключевые слова: прыжки с трамплина, аэродинамические коэффициенты, полёт, оптимизация

Received 28 May 2002